FEBS Letters 587 (2013) 770–774

FEBS Letters

journal homepage: www.FEBSLetters.org

The heme-copper oxidase superfamily shares a Zn^{2+}-binding motif at the entrance to a proton pathway

Hyun Ju Lee [1], Pia Ädelroth *

Department of Biochemistry and Biophysics, The Arrhenius Laboratories for Natural Sciences, Stockholm University, SE-106 91 Stockholm, Sweden

ARTICLE INFO

Article history:
Received 6 December 2012
Revised 30 January 2013
Accepted 31 January 2013
Available online 8 February 2013

Edited by Stuart Ferguson

Keywords:
cbb_3
Proton transfer
K-pathway
Nickel
Liposome
Nitric oxide reductase

ABSTRACT

Heme-copper oxidases (HCuOs) catalyse the reduction of oxygen, using the liberated free energy to maintain a proton-motive force across the membrane. In the mitochondrial-like A-type HCuOs, binding of heavy metal ions at the surface of the protein inhibits proton transfer. In bacterial C-type oxidases, the entry point to the proton pathway is on an accessory subunit unrelated to any subunit in A-type HCuOs. Despite this, we show here that heavy metal ions such as Zn^{2+} inhibit O_2-reduction very similarly in C-type as in A-type HCuOs, and furthermore that the binding site shares the same Glu-His motif.

1. Introduction

Heme-copper oxidases (HCuOs) are integral membrane proteins that form the last component of the respiratory chain, catalysing the reduction of oxygen to water (see Eq. (1)). All HCuOs have a homologous catalytic subunit with twelve transmembrane helices harbouring six invariant histidines which ligate three cofactors; a high-spin heme and a copper ion (Cu_B) in the catalytic site and an additional low-spin heme. HCuOs conserve energy from O_2-reduction by generating a proton electrochemical gradient across the membrane. This is achieved by using electrons from donors in the 'outside' solution and protons from the 'inside' of the membrane, and also by translocating protons across the membrane. In the mitochondrial-like A-type HCuOs, four protons are translocated across the membrane for every oxygen reduced to water (i.e. in Eq. (1), $n = 4$).

$$O_2 + 4\ e^-_{out} + (4+n)H^+_{in} \rightarrow 2H_2O + nH^+_{out} \quad (1)$$

The HCuO superfamily is classified into three major subfamilies denoted A-, B-, and C-type [1,2], and also bacterial NO-reductases (NOR) belong to the HCuO family (see below), where they form their own subfamily.

In the mitochondrial-like, or A-type HCuOs, the catalytic subunit I contains the Cu_B, the low-spin heme *a* and the high-spin heme a_3. There is an additional redox cofactor, Cu_A, bound to subunit II, a membrane-anchored protein. Cu_A is the acceptor of electrons from the donor, soluble cyt. *c*. Protons are transferred through two defined pathways (see [3] for a recent review on proton pathways in the HCuO family) up to the catalytic site, the D- and the K-pathway. The D-pathway is the main pathway for both chemical and pumped protons (in total 6–7 H^+ per O_2). The K-pathway is used for protons (1–2) taken up during the reduction of the active site and starts with a glutamate in subunit II ($E101^{II}$ in *Rhodobacter sphaeroides* aa_3) [4,5], which is the only residue in either the D- or K-pathways not found in subunit I.

The B- and C-type HCuOs differ from the A-type in that the D-pathway is missing in the sequence, and they presumably use only one proton transfer pathway, analogous in its spatial location to the K-pathway [2,6].

The C (cbb_3) family of oxidases are found exclusively in bacteria, and is the O_2-reducing HCuO most distantly related to the A-type, and the closest to NOR. The C-type HCuO from *Pseudomonas stutzeri* was recently structurally defined at atomic resolution [7]. In C-type HCuOs, the catalytic subunit CcoN, related to subunit I of the A- and B-type, contains the high-spin heme b_3-Cu_B catalytic

Abbreviations: HCuO, heme-copper oxidase; NOR, bacterial nitric oxide reductase; *c*NOR, cytochrome *c*-dependent NOR; DDM, β-D-dodecyl maltoside; TMPD, *N,N,N′,N′*-tetramethyl-*p*-phenylenediamine; FCCP, carbonyl cyanide-*p*-trifluoromethoxyphenyl-hydrazon; RCR, respiratory control ratio

* Corresponding author. Fax: +46 8 153679.
E-mail address: piaa@dbb.su.se (P. Ädelroth).
[1] Current address: Department of Mitochondrial Genetics, Max Planck Institute for Biology of Ageing, Cologne, Germany.

0014-5793/$36.00
http://dx.doi.org/10.1016/j.febslet.2013.01.069

site and a low-spin heme *b*. CcoO is a membrane-anchored protein containing one *c*-type heme and has no counterpart in other O_2-reducing HCuOs, but is related to NorC in NOR. CcoP, also anchored to the membrane via one trans-membrane helix, contains two *c*-type hemes and has no counterpart in any other HCuO.

The K-pathway analogue in C-type HCuOs was suggested [7] to start at the Glu-49 (*P. stutzeri* cbb_3 numbering) in CcoP. We recently showed that this Glu (Glu-25^P in *R. sphaeroides* cbb_3) is needed for efficient proton transfer [8], thus identifying it as a crucial part of the proton transfer pathway. The Glu-49 in CcoP is also here the only residue in the proton pathway not located in CcoN. Thus, all O_2-reducing HCuO subfamilies have the entry point to the K-pathway (analogue) in one of the accessory subunits.

Bacterial NO-reductases (NOR) also belong to the HCuO superfamily, although their physiological role is to reduce NO to N_2O. In the best characterised NORs, the *c*NORs, one major difference to the O_2-reducing HCuOs is that NO-reduction, although as exergonic as O_2-reduction, is non-electrogenic and protons and electrons are derived from the same side of the membrane (see [3] and references therein). Hence, *c*NOR has neither a D- nor a K-pathway analogue, as confirmed by the crystal structure of *c*NOR from *Pseudomonas aeruginosa* [9].

Many proton-transferring membrane proteins, e.g. the bacterial photosynthetic reaction center (RC) are inhibited by heavy metal cations such as Zn^{2+}, Ni^{2+} and Cd^{2+} [10]. This presumably occurs because the metals tend to bind to acidic and histidine residues found at the entry point to the proton-transferring pathways (where they form a 'proton-collecting antenna' [11]). In A-type HCuOs, Zn^{2+} has been shown to inhibit catalytic turnover [12,13], proton transfer during oxidation [14], release of pumped protons [15] and to decrease the pumping stoichiometry [15,16]. Also, other heavy metal ions such as Cd^{2+} and Ni^{2+} inhibit O_2-reduction in A-type HCuOs [12].

In a crystal structure of the A-type HCuO from *R. sphaeroides*, binding of Cd^{2+} was observed at the entrance to the K-pathway, where it was ligated by Glu-101^{II} and a nearby histidine on the same subunit, H-96^{II} [17]. In a crystal of the bovine oxidase soaked with Cd^{2+} or Zn^{2+}, the metals were found bound to a His at the entrance to the D-pathway [18].

In C-type HCuOs, there is no evolutionary relationship between the CcoO or CcoP with the subunits II or III in A-type HCuOs. Despite this, the arrangement of histidines surrounding the glutamic acid at the entry point to the K-pathway analogue is similar to that found in the A-type. In this work, we have investigated the effect of heavy metal ions on catalytic turnover in the C-type (cbb_3) from *R. sphaeroides*. Our results show that the inhibition pattern of Zn^{2+} and Ni^{2+} is very similar between the A- and C-type HCuOs, and that furthermore, a histidine (His-18^P) in the CcoP subunit close to the Glu (Glu-25^P) that defines the proton entry point is part of the metal binding site.

2. Materials and methods

2.1. Construction of site-directed mutant forms and protein purification

Construction of E25^{P}A and E25^{P}Q was described earlier [8]. Both H18^{P}A and H124^{N}A were constructed in the same manner as in [8]. Briefly, the ccoNOPQ fragment (BamHI-EcoRI) from pUI2803NHIS subcloned to pBluescript SK+ was used for site directed mutagenesis with the Quikchange kit (Stratagene). Mutagenic primers were from Eurofins, restriction enzymes from Fermentas, and sequencing performed by Eurofins. The ccoNOPQ containing the mutation was ligated back to pRK-415. The plasmid containing the mutation was transformed into S-17-1, and finally transferred into the *R. sphaeroides* Δcbb_3 strain by conjugation. The *R. sphaeroides* Δcbb_3 strain carrying the plasmid pUI2803NHIS [19] with mutations were grown, and the cbb_3 wildtype and variants were purified as in [8]. The growth of *Escherichia coli* expressing *c*NOR and its purification was done as in [20].

2.2. Steady-state activity measurements and data handling

The steady-state O_2-reduction activity of cbb_3 was measured using a Clark-type electrode (Hansatech). The reaction chamber was filled (total of 1 ml) with 50 mM Hepes-KOH, pH 7.4, 50 mM KCl, 0.03% β-D-dodecyl maltoside (DDM), 5 mM ascorbate, 0.5 mM *N*,*N*,*N*′,*N*′-tetramethyl-*p*-phenylenediamine (TMPD), and 20–40 μM horse heart cytochrome *c*. For measurements with cbb_3–liposomes 100 mM Hepes-KOH at pH 7.4 was used.

$ZnSO_4$–$7H_2O$ (Sigma), $NiSO_4$–$6H_2O$ (Sigma), and $CaCl_2$–$2H_2O$ (Scharlan) were used for metal stock solutions and prepared by serial dilutions. Na–EDTA (Scharlan) at pH 7.4 was used as a chelator. The metal solutions were added directly to the measuring chamber after the addition of cbb_3. A few subsequent additions of metal solution were made, followed by addition of excess EDTA before the measurement was repeated. Because of the limited solubility of $Zn(OH)_2$ at pH > 7 [21], we did not use Zn^{2+}-concentrations above 0.5 mM when fitting the data.

The effect of metals added on the turnover activity of cbb_3 was fitted, as in [12], to Eq. (2) using Sigmaplot (Systat Software):

$$V_{obs} = \frac{V_0}{1 + [M^{2+}]/K_i} \quad (2)$$

If the fit was not satisfactory, a background rate V_b was added to the equation to account for a non-zero turnover rate at high metal ion concentration. Alternatively, the data obtained was fitted to two inhibitory sites [12] according to Eq. (3):

$$V_{obs} = \frac{V_0^1}{1 + [M^{2+}]/K_i^1} + \frac{V_0^2}{1 + [M^{2+}]/K_i^2} \quad (3)$$

2.3. Reconstitution of the cbb_3 into phospholipid vesicles

Purified soybean lipids (L-α-phosphatidylcholine, Sigma–Aldrich, 40 mg/ml) in 2% cholate, 100 mM Hepes-KOH, pH 7.4 were mixed and sonicated. The *R. sphaeroides* cbb_3 was then added and the mixture incubated in room temperature for one hour with occasional shaking. The mixture was then passed through a PD-10 column (GE Healthcare) resulting in incorporation of the cbb_3 into small unilamellar vesicles (see [22]). The respiratory control ratio (RCR, see also [8]) was measured as the ratio of the rates of O_2-reduction after and before the addition of valinomycin/carbonyl cyanide-*p*-trifluoromethoxyphenyl-hydrazon (FCCP). The RCR was typically above 6, indicating that the vesicles prepared by this method are well sealed. The absolute turnover activity in uncontrolled vesicles was similar to that in the solubilised enzyme.

3. Results

3.1. Turnover oxygen reduction activity in *R. sphaeroides* cbb_3 variants

Both the H214^{N}A and H18^{P}A variants show high O_2-reduction turnover, with 120% and 90% of the wildtype activity, respectively.

3.2. Metal ion inhibition of O_2-turnover in solubilised cbb_3 and cNOR

Zn^{2+} affects the rate of O_2-reduction in cbb_3, a titration of observed turnover rate versus added Zn^{2+} is shown in Fig. 1. Ni^{2+} also inhibits turnover, whereas Ca^{2+} shows very little inhibition. The K_is

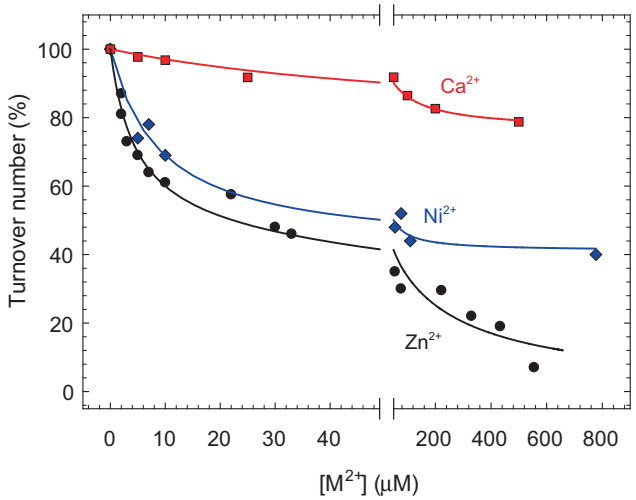

Fig. 1. Metal inhibition on O_2-reduction turnover in *cbb*$_3$. Black dots for Zn^{2+}, blue diamonds for Ni^{2+} and red squares for Ca^{2+}. The respective lines are fits to the data, for Zn^{2+} the obtained K_is (see Section 2) were: 4.5 μM/230 μM, for Ni^{2+}: 9 μM and for Ca^{2+}: 70 μM.

obtained from the fits shown in Fig. 1 are tabulated in Table 1. Zn^{2+} binding occurs with two different affinities, where the first is well-defined, with a K_i of 4.5 μM, but the second occurs around 200 μM, and obtained relative inhibition varied somewhat between experiments (as evidenced by the higher degree of scattering at higher Zn^{2+} in Fig. 1). Data shown for Zn^{2+} and Ni^{2+} are data combined from at least 4 different independent experiments (see Section 2). The observed effects were reversible by the addition of excess EDTA.

In *c*NOR, where there is no K-pathway analogue, we also observe metal inhibition on O_2 reduction turnover (see Table 1), but to a much smaller degree, and there is little difference between Zn^{2+}, Ni^{2+} and Ca^{2+}.

3.3. Zn^{2+} and Ni^{2+} inhibition in *cbb*$_3$ variants

Zn^{2+} and Ni^{2+} inhibition on turnover was measured in the E25^{P}A, E25^{P}Q, H18^{P}A and H214A. Results are presented in Table 1 and for H18^{P}A also in Fig. 2. Of these variant *cbb*$_3$, the most significant effect was observed with the H18^{P}A, which showed roughly a 10-fold increase in the K_i for both Zn^{2+} and Ni^{2+}.

3.4. Zn^{2+} and Ni^{2+} inhibition on turnover in liposome-reconstituted *cbb*$_3$

Zn^{2+} affects also the O_2-reduction activity of *cbb*$_3$ reconstituted into lipid vesicles, in a manner qualitatively very similar to what is found with the A-type HCuO from *R. sphaeroides* [12]. In the

Table 1
Zn^{2+} and Ni^{2+} inhibition on O_2-reduction in solubilised *cbb*$_3$ variants and *c*NOR.

Enzyme variant	Corresponding residue in *P. stutzeri cbb*$_3$	Activity e^-s^{-1}	Zn^{2+} K_i (μM)	Ni^{2+} K_i (μM)
Wt *cbb*$_3$		200 (100%)	4.5/~200	9
H214^{N}A *cbb*$_3$	H156^N	230 (115%)	5	10
H18^{P}A *cbb*$_3$	H42^P	180 (90%)	40	75
E25^{P}A *cbb*$_3$	E49^P	13 (6%), data from [8]	7	22
E25^{P}Q *cbb*$_3$		10 (5%), data from [8]	10	24
*c*NOR wt		~5	130	20[a]

[a] Resulting in less than 30% inhibition.

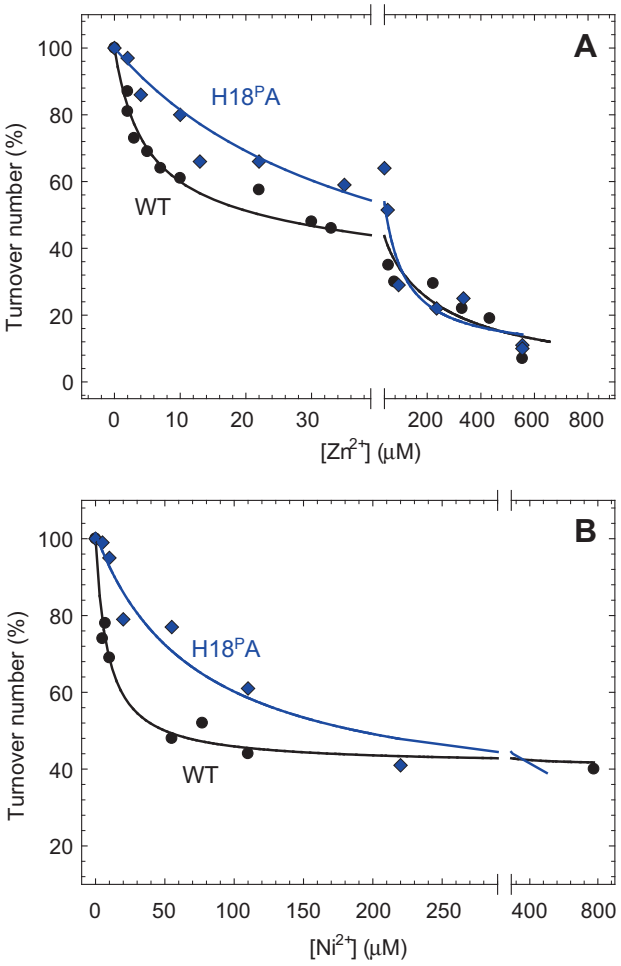

Fig. 2. Zn^{2+} (A) and Ni^{2+} (B) inhibition in the H18^{P}A (corresponding to H42^P in *P. stutzeri*) *cbb*$_3$ variant compared to WT. For the H18^{P}A, the inhibition patterns was fitted (blue lines) to one inhibitory site with K_is of 40 μM for Zn^{2+} and 75 μM for Ni^{2+}.

controlled liposome-reconstituted *cbb*$_3$, we obtain a K_i for Zn^{2+} of 12 μM (see Fig. 3) on the O_2-reduction activity and in the uncontrolled state (after addition of the uncouplers valinomycin and FCCP) the K_i increases to 130 μM. For Ni^{2+}, the obtained K_is were 9 μM (controlled) and 20 μM (uncontrolled). However, preliminary data for Zn^{2+} inhibition indicate that if the turnover activity in the uncontrolled state is made as slow as in the controlled state by reducing the concentration of the mediator TMPD, the observed K_i decreases to a value similar to that observed in the controlled state (see Section 4). Also in *cbb*$_3$–liposomes, Ca^{2+} shows a very small inhibition similar to that observed in the solubilised enzyme (data not shown). The observed effects were all reversible by addition of excess EDTA.

4. Discussion

The K-pathway (analogue) for proton transfer is conserved throughout the O_2-reducing HCuOs (but not to *c*NOR), even though the residues are not conserved, the location is. This pathway has as its entry point a glutamic acid in an accessory subunit, which is a recurring feature [4–6,8,23] as the subunits are evolutionary unrelated. In *R. sphaeroides aa*$_3$, close to this glutamate (Glu-101^{II}) is a histidine (H-96^{II}), that together with the Glu forms a binding site for Cd^{2+}, as observed in the crystal structure obtained with Cd^{2+} [17]. When the Glu-101^{II} and His-96 are exchanged (Glu-101^{II}A/His-96^{II}A double mutant) for alanines, metal binding

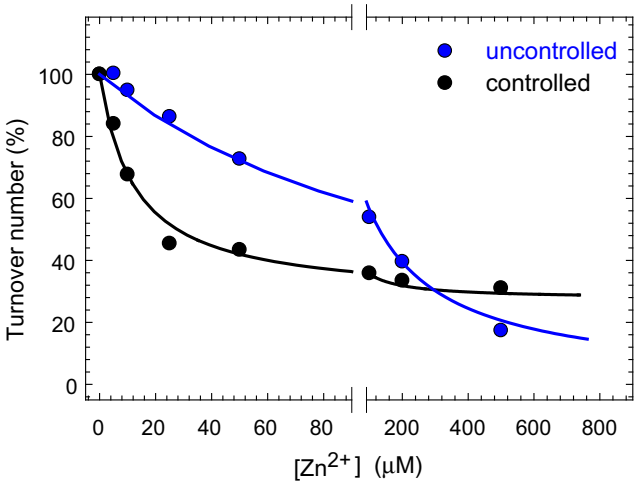

Fig. 3. The effect of Zn^{2+} on the O_2-reduction activity in liposome-reconstituted *cbb*$_3$ in the controlled (black) and uncontrolled (after addition of the uncouplers valinomycin and FCCP, blue) states. The black and blue lines are fits to the data, with K_is thus obtained 12 μM for the controlled, and 130 μM for the uncontrolled. 100% activity corresponds to ~180 e^-s^{-1} and 30 e^-s^{-1} for uncontrolled and controlled, respectively.

is severely diminished, as evidenced by the effects on the K_is for Zn^{2+} on O_2 turnover [23]. In the crystal structure of *cbb*$_3$ (C-type) from *P. stutzeri* [7], close to the Glu-49^P in the CcoP subunit that forms the proton entry point [8] there are two histidines within 10 Å distance; His-42^P in CcoP and His-156 in CcoN, as shown in Fig. 4. In a limited alignment of about 40 *cbb*$_3$ sequences from different bacteria, these histidines are mostly, if not fully, conserved. As shown in this work, mutating any one of these histidines (in the *R. sphaeroides cbb*$_3$) to alanines, has no effect on O_2 turnover, showing that neither of them alone has a crucial role for proton transfer. However, the K_i for both Zn^{2+} and Ni^{2+} binding is increased about an order of magnitude in the H18^{P}A (corresponding to H42^P in *P. stutzeri*), showing that this His is involved in the binding of both these metal ions, and that the metal ion inhibition mechanism presumably involves a decrease in the rate of proton transfer into the K-pathway analogue. There was no effect on metal ion binding in the H214A variant (corresponding to His-156 in *P. stutzeri*). We note that the His-42^P and the Glu-49^P are somewhat too far apart (~10 Å) in the crystal structure to form a metal binding site, but a similar situation is observed in *R. sphaeroides aa*$_3$, where the His-96^{II} is 7–10 Å away from the Glu-101^{II} in the original structure (pdb ID 1M56 [24]), but moves closer (Glu-His distance 4–5 Å with Cd^{2+} in between) when Cd^{2+} is bound (pdb ID 2GSM[17]). It is thus possible that a similar structural change occurs upon metal binding in *cbb*$_3$.

In the E25^{P}A (corresponding to the Glu-49^P in *P. stutzeri*) and E25^{P}Q variants, there is a 2-fold increase in the K_i for Ni^{2+}, but no significant effect on the K_i for Zn^{2+}. It is somewhat surprising that we do not see an effect on the K_i for Zn^{2+} in these variants, as the binding site, in analogy with *aa*$_3$ should involve this Glu. However, as discussed previously [8], turnover is very slow in these variants, and limited by proton transfer, which is presumably not the case in the WT, which means that these variants might initially be more sensitive to additional slowing of proton transfer by Zn^{2+} binding. Also, similarly to the effects seen in liposomes, the rates at which intermediates form and decay might in itself affect their sensitivity to Zn^{2+}. Without knowing the exact mechanism of metal inhibition, interpreting data from variants with drastically different turnover rates (see Table 1) is difficult.

We note that although the arrangement with histidine residues around the acidic residue that forms the entry point to the proton transfer pathway is a feature found across the O_2-reducing HCuOs

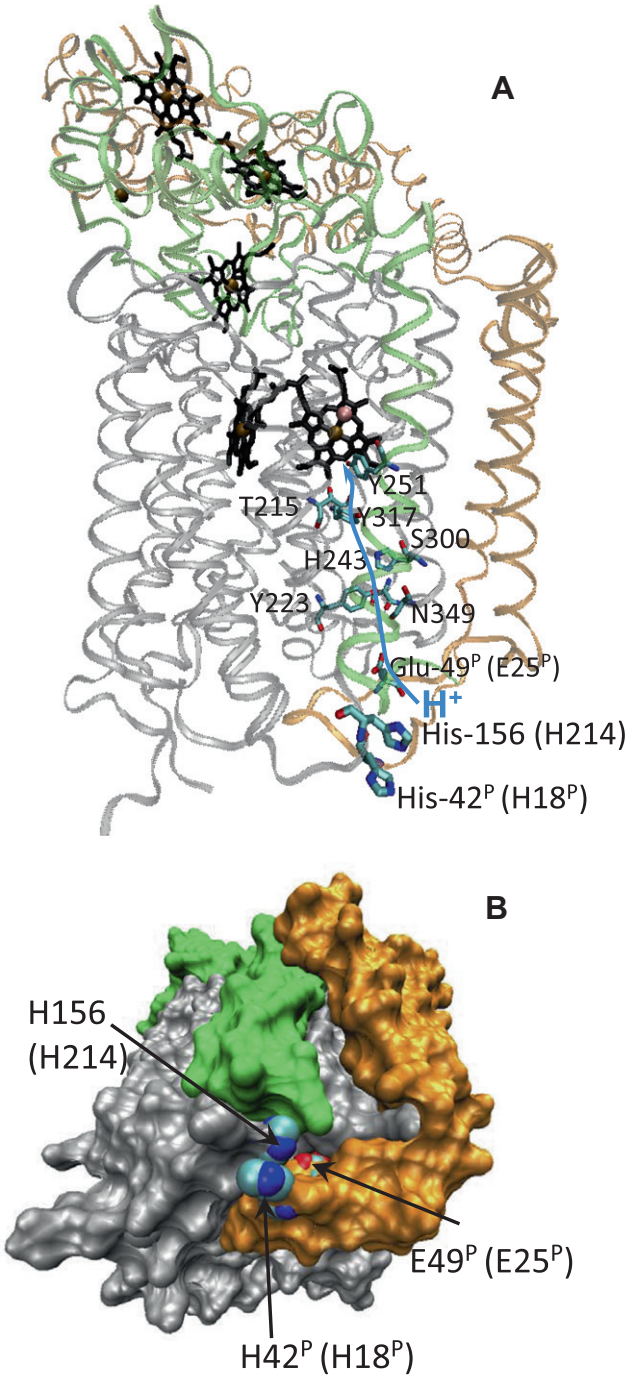

Fig. 4. Structure of the *cbb*$_3$ from *P. stutzeri* (PDB ID 3MK7 [7]). Shown in A is an overview of CcoN (grey), CcoO (green) and CcoP (orange) with the K-proton pathway analogue indicated. The surface histidines His-42^P and His-156 are highlighted. Numbering of the corresponding residues in the *R. sphaeroides cbb*$_3$ are indicated (in parenthesis) for those discussed in this work. Unless otherwise indicated (for Glu-49^P and His-42^P), the residues are all in CcoN. In B is shown a surface representation viewed from 'underneath' showing the surface location of the histidines and the partially surface-exposed Glu-49^P. Colour-coding of the subunits as in A. The figure was made using the VMD software [26].

as well as in bacterial RCs, these histidines are in themselves not crucial for providing proton transfer rapid enough not to be limiting for turnover at the conditions tested. This is shown for the His-18^P in this work, and is reminiscent of the situation in bacterial RCs, where there are two His residues at the entry point to the proton transfer pathway, that are both involved in metal ion binding. Exchanging any one of these His to Ala has no observed effect on

the proton transfer rate, but only when both are exchanged is the observed proton transfer rate slowed [25].

It is at this point not clear to us what the mechanism of metal ion inhibition on liposome-reconstituted cbb_3 is. The pattern with a much more pronounced effect in the controlled, as compared to the uncontrolled state (see Fig. 3), is very similar to the situation in the *R. sphaeroides* aa_3 [12], where this was interpreted as being due to metal ion inhibition on the 'back leak' proton pathway, and this might be the case also in cbb_3. The pathway for pumped protons leading to the 'outside' is not well defined in any HCuO. However, our preliminary data in liposomes where we matched the turnover number with uncontrolled cbb_3 to that observed in the controlled state indicates that the difference is related to the turnover rates, possibly due to binding of Zn^{2+} to a specific intermediate, as discussed for the bovine oxidase, where the Zn^{2+} inhibition was equally strong in the uncontrolled state if the vesicles were pre-incubated with Zn^{2+} [13]. We did not pursue this issue further at this point as the main point of this study was to show that the metal ion inhibition is observed also in the C-type HCuOs and to identify the inhibitory site at the K-pathway entrance.

In summary, we have shown that the C-type HCuO from *R. sphaeroides* is inhibited by Zn^{2+} in a manner very similar to that found with A-type oxidases, and that the binding site for Zn^{2+} involves the same arrangement of a His residue close to the Glu that forms the entry point to the K-pathway analogue. This Zn^{2+}-binding motif recurs in evolutionary unrelated proteins, and is an example of convergent evolution that shows that the arrangement of acidic and histidine residues forming a 'proton-collecting' antenna presumably provides advantages for rapid proton transfer.

Acknowledgements

H.J.L. was supported by a post-doctoral stipend from the Wenner-Gren foundation when these studies were initiated. P.Ä. is a Royal Swedish Academy of Sciences Research Fellow supported by a grant from the Knut and Alice Wallenberg Foundation. This work was funded by a grant from the Swedish Research Council (VR). We thank Josy ter Beek for the sample of *c*NOR.

References

[1] Sousa, F.L., Alves, R.J., Pereira-Leal, J.B., Teixeira, M. and Pereira, M.M. (2011) A bioinformatics classifier and database for heme-copper oxygen reductases. PLoS One 6, e19117.
[2] Hemp, J., Han, H., Roh, J.H., Kaplan, S., Martinez, T.J. and Gennis, R.B. (2007) Comparative genomics and site-directed mutagenesis support the existence of only one input channel for protons in the C-family (cbb(3) oxidase) of heme-copper oxygen reductases. Biochemistry 46, 9963–9972.
[3] Lee, H.J., Reimann, J., Huang, Y. and Ädelroth, P. (2012) Functional proton transfer pathways in the heme-copper oxidase superfamily. Biochim. Biophys. Acta 1817, 537–544.
[4] Brändén, M., Tomson, F., Gennis, R.B. and Brzezinski, P. (2002) The entry point of the K-proton-transfer pathway in cytochrome c oxidase. Biochemistry 41, 10794–10798.
[5] Ma, J. et al. (1999) Glutamate-89 in subunit II of cytochrome bo3 from *Escherichia coli* is required for the function of the heme-copper oxidase. Biochemistry 38, 15150–15156.
[6] Chang, H.Y., Hemp, J., Chen, Y., Fee, J.A. and Gennis, R.B. (2009) The cytochrome ba3 oxygen reductase from *Thermus thermophilus* uses a single input channel for proton delivery to the active site and for proton pumping. Proc. Natl. Acad. Sci. USA 106, 16169–16173.
[7] Buschmann, S., Warkentin, E., Xie, H., Langer, J.D., Ermler, U. and Michel, H. (2010) The structure of cbb3 cytochrome oxidase provides insights into proton pumping. Science 329, 327–330.
[8] Lee, H.J., Gennis, R.B. and Ädelroth, P. (2011) Entrance of the proton pathway in cbb3-type heme-copper oxidases. Proc. Natl. Acad. Sci. USA 108, 17661–17666.
[9] Hino, T., Matsumoto, Y., Nagano, S., Sugimoto, H., Fukumori, Y., Murata, T., Iwata, S. and Shiro, Y. (2010) Structural basis of biological N_2O generation by bacterial nitric oxide reductase. Science 330, 1666–1670.
[10] Axelrod, H.L., Abresch, E.C., Paddock, M.L., Okamura, M.Y. and Feher, G. (2000) Determination of the binding sites of the proton transfer inhibitors Cd^{2+} and Zn^{2+} in bacterial reaction centers. Proc. Natl. Acad. Sci. USA 97, 1542–1547.
[11] Marantz, Y., Nachliel, E., Aagaard, A., Brzezinski, P. and Gutman, M. (1998) The proton collecting function of the inner surface of cytochrome c oxidase from *Rhodobacter sphaeroides*. Proc. Nat. Acad. Sci. USA 95, 8590–8595.
[12] Mills, D.A., Schmidt, B., Hiser, C., Westley, E. and Ferguson-Miller, S. (2002) Membrane potential-controlled inhibition of cytochrome c oxidase by zinc. J. Biol. Chem. 277, 14894–14901.
[13] Vygodina, T.V., Zakirzianova, W. and Konstantinov, A.A. (2008) Inhibition of membrane-bound cytochrome c oxidase by zinc ions: high-affinity Zn^{2+}-binding site at the P-side of the membrane. FEBS Lett. 582, 4158–4162.
[14] Aagaard, A., Namslauer, A. and Brzezinski, P. (2002) Inhibition of proton transfer in cytochrome c oxidase by zinc ions: delayed proton uptake during oxygen reduction. Biochim. Biophys. Acta 1555, 133–139.
[15] Faxén, K., Salomonsson, L., Ädelroth, P. and Brzezinski, P. (2006) Inhibition of proton pumping by zinc ions during specific reaction steps in cytochrome c oxidase. Biochim. Biophys. Acta 1757, 388–394.
[16] Kannt, A., Ostermann, T., Müller, H. and Ruitenberg, M. (2001) Zn(2+) binding to the cytoplasmic side of *Paracoccus denitrificans* cytochrome c oxidase selectively uncouples electron transfer and proton translocation. FEBS Lett. 503, 142–146.
[17] Qin, L., Hiser, C., Mulichak, A., Garavito, R.M. and Ferguson-Miller, S. (2006) Identification of conserved lipid/detergent-binding sites in a high-resolution structure of the membrane protein cytochrome c oxidase. Proc. Natl. Acad. Sci. USA 103, 16117–16122.
[18] Muramoto, K., Hirata, K., Shinzawa-Itoh, K., Yoko-o, S., Yamashita, E., Aoyama, H., Tsukihara, T. and Yoshikawa, S. (2007) A histidine residue acting as a controlling site for dioxygen reduction and proton pumping by cytochrome c oxidase. Proc. Natl. Acad. Sci. USA 104, 7881–7886.
[19] Oh, J.I. and Kaplan, S. (2002) Oxygen adaptation. The role of the CcoQ subunit of the cbb3 cytochrome c oxidase of *Rhodobacter sphaeroides* 2.4.1. J. Biol. Chem. 277, 16220–16228.
[20] Flock, U., Thorndycroft, F.H., Matorin, A.D., Richardson, D.J., Watmough, N.J. and Ädelroth, P. (2008) Defining the proton entry point in the bacterial respiratory nitric-oxide reductase. J. Biol. Chem. 283, 3839–3845.
[21] Cherny, V.V. and DeCoursey, T.E. (1999) PH-dependent inhibition of voltage-gated H+ currents in rat alveolar epithelial cells by Zn2+ and other divalent cations. J. Gen. Phys. V114, 819–838.
[22] Wiedenmann, A., Dimroth, P. and von Ballmoos, C. (2008) Deltapsi and DeltapH are equivalent driving forces for proton transport through isolated F(0) complexes of ATP synthases. Biochim. Biophys. Acta 1777, 1301–1310.
[23] Qin, L., Mills, D.A., Hiser, C., Murphree, A., Garavito, R.M., Ferguson-Miller, S. and Hosler, J. (2007) Crystallographic location and mutational analysis of Zn and Cd inhibitory sites and role of lipidic carboxylates in rescuing proton path mutants in cytochrome c oxidase. Biochemistry 46, 6239–6248.
[24] Svensson-Ek, M., Abramson, J., Larsson, G., Törnroth, S., Brzezinski, P. and Iwata, S. (2002) The X-ray crystal structures of wild-type and EQ(I-286) mutant cytochrome c oxidases from *Rhodobacter sphaeroides*. J. Mol. Biol. 321, 329–339.
[25] Ädelroth, P., Paddock, M.L., Tehrani, A., Beatty, J.T., Feher, G. and Okamura, M.Y. (2001) Identification of the proton pathway in bacterial reaction centers: decrease of proton transfer rate by mutation of surface histidines at H126 and H128 and chemical rescue by imidazole identifies the initial proton donors. Biochemistry 40, 14538–14546.
[26] Humphrey, W., Dalke, A. and Schulten, K. (1996) VMD: visual molecular dynamics. J. Mol. Graph. 14, 33–38.